

Formulation, Optimization, and Evaluation of Gliclazide loaded Nanosuspension for Dissolution Rate Enhancement

Padmnabh*, DC Bhatt

Department of Pharmaceutical Sciences, Guru Jambheshwar University of Science and Technology, Hisar, Haryana, India.

Received: 10th October, 2023; Revised: 02nd November, 2023; Accepted: 16th November, 2023; Available Online: 25th December, 2023

ABSTRACT

Diabetes mellitus is a prolonged metabolic condition categorized through elevated blood glucose levels. To treat this condition, oral antihyperglycemic medications like gliclazide, a second-generation sulfonylurea insulin secretagogue, are commonly used. Gliclazide comes into the biopharmaceutical classification system (BCS) class-II types, known for its lower solubility. To enhance its solubility, gliclazide was integrated into nanosuspensions. This study focused on formulating these gliclazide nanosuspensions using Kollicoat IR and Soluplus through the anti-solvent-precipitation method, through optimization achieved using the Box Behnken Design. Key parameters assessed included particle size (224 ± 1.23 nm) and entrapment efficiency ($95.65 \pm 0.12\%$). The drug release studies conducted on pH 7.4 indicated that over 95% of the drug was released within 30 minutes for the nanosuspension, whereas the pure drug solution released less than 70% in the same time frame, indicating immediate release with the nanosuspension. The morphology was examined using scanning electron microscopy (SEM), while fourier transform infrared (FTIR), X-Ray diffractometers (XRD), and differential scanning calorimeter (DSC) analyses confirmed the presence of the drug within the nanosuspension. In summary, the incorporation of gliclazide into nanosuspensions proved successful, resulting in enhanced release characteristics and ameliorated solubility.

Keywords: Nanosuspensions, Solubility, Diabetes, Optimization.

International Journal of Pharmaceutical Quality Assurance (2023); DOI: 10.25258/ijpqa.14.4.45

How to cite this article: Padmnabh, Bhatt DC. Formulation, Optimization, and Evaluation of Gliclazide loaded Nanosuspension for Dissolution Rate Enhancement. International Journal of Pharmaceutical Quality Assurance. 2023;14(4):1107-1114.

Source of support: Nil.

Conflict of interest: None

INTRODUCTION

Diabetes mellitus is a prolonged metabolic ailment that has substantial social, health, in addition to financial consequences.¹ However, the characterization is based on the glucose concentrations in blood, such as high blood glucose levels leading to the symptoms of hyperglycemia, which is considered one of the diabetes mellitus conditions.² While insulin resistance typically coexists with these metabolic disorders. Hyperglycemia is well-known as non-insulin-dependent diabetes mellitus and it is a complex condition that primarily affects adults.^{3,4} Furthermore, oral antihyperglycemic drugs are utilized to treat this disease, such as the sulfonylurea class of insulin secretagogues gliclazide (second-generation drug of sulfonylureas), which stimulates the β -cell receptor.^{5,6} Even increased the release of basal and meal-stimulated insulin, enhanced peripheral glucose uptake, and decreased hepatic gluconeogenesis.^{7,8} The primary action of gliclazide is to connect with ATP-sensitive potassium channel receptors, lowering potassium conductance, and causing membrane depolarization.⁹ This action raises intracellular calcium ion concentration and triggers the release of insulin. Alongside there are a number of drawbacks that were

visualized in conventional drugging delivery systems such as systemic side effects, and low bioactivity.¹⁰ In order to achieve these drawbacks, the nanoparticle system was introduced such as nanosuspensions, these are colloidal systems comprising stabilizers and pure drugs, either in their original form or as freeze-dried into a solid matrix. Nanosuspensions in both organic and aqueous phases are employed to improve the solubility of drugs.¹¹⁻¹³ Nanosuspensions, often referred to as particles resembling fine dust, aid in the dissolution of a scheme and enhance absorption, promoting increased effectiveness.¹⁴ Moreover, it demonstrated the photostability, stability at room temperature in addition to humidity, and compatibility using the excipient and solvent.¹⁵ However, for chemicals with a higher log *p*-value, higher melting point, as well as higher dosages that are insoluble in water but soluble in oil; nanosuspension is favored.¹⁶ Additionally, API that are unsolvable in together water and organic solvents can also be employed with nanosuspension expertise including biopharmaceutical classification system (BCS) class-II or IV drugs such as gliclazide can be utilized to encapsulate in nanosuspension to enhance the solubility and side effects.^{17,18} In this review, we discussed the sulfonylureas class gliclazide

*Author for Correspondence: padmanabhkm@gmail.com

for the management of diabetes mellitus to reduce its side effects and enhancement its solubility thus, loaded in the nanosuspension.

MATERIALS AND METHOD

Materials

Gliclazide was acquired as a gifted specimen commencing Tiruvision Medicare, Baddi, Sodium lauryl sulphate (SLS) was procured from Lobagens, Kollicoat IR and Soluplus was gift sample from BASF, DMSO purchased from Blessed Organics. All supplementary chemicals and reagents were used of analytical grade.

Method

Formulation of nanosuspensions of gliclazide

Nanosuspensions of gliclazide were formulated through the precipitation-ultrasonication method. Briefly, gliclazide was dissolved using DMSO as the solvent. While Kollicoat IR, Soluplus and SLS were dissolved in water using a magnetic stirrer at 1500 rpm to act as an anti-solvent solution precooled to 4°C. After that, the drug's solvent mixture was added dropwise into the antisolvent mixture comprising polymers and surfactants. The created suspension was then subjected to the ultrasonication probe's treatment creating the ideal nano sizes, the formulated nanosuspensions were centrifugated at optimum rpm for a sufficient time. Moreover, after the centrifugation, the supernatant was discarded and the rest sediments or the solid residue was dehydrated in hot air oven at 40°C for a sufficient time. The formulated nanosuspensions of gliclazide were evaluated on numerous process parameters including particle size, entrapment efficiency, and furthermore.¹⁹⁻²¹

Optimization of nanosuspensions of gliclazide

Using the Box-Behnken experimental methods, the nanosuspension formulation's statistical optimization was completed. Particle size (Y1), entrapment efficiency (Y2), and drug release (Y3) were the dependent variables, whereas the amounts of the soluplus (X1), kollicoat (X2), as well as sonication time (X3) were the independent factors for optimization.²² In a multidimensional cube, the Box-Behnken design sets a point in triplicate at the center and at the middle of each edge. The Table 1 shows the lower (-1), middle (0), and higher (+1) levels of the independent variables, which were assessed and established on the results of the early experiments. The table also displays the response criteria (i.e., the dependent variables, Y1) for the optimization of the formulation. As indicated in the table, design matrices with 17 trial runs were produced using the Design Expert summarized in Table 1.²³

Evaluation of nanosuspensions of gliclazide

• Particle size, and %EE

The Malvern Zetasizer (Nano ZS 90, Malvern Instruments, UK) was utilized to measure the particle size (nm), as well as PDI at 25°C. Double-distilled water was used to adequately dilute the nanosuspension dispersion before measurement. Non-encapsulated drug was determined using the supernatant

Table 1: Low, medium, and high stages of the independent variables

| Independent variables | Levels | | |
|--|---------------------------------------|--------|------|
| | Low | Medium | High |
| X ₁ = Soluplus (mg) | 95 | 105 | 115 |
| X ₂ = Kollicoat (mg) | 95 | 105 | 115 |
| X ₃ = Sonication time (minutes) | 10 | 15 | 20 |
| Transformed Values | -1 | 0 | +1 |
| Dependent Variables | Y ₁ = Particle size (nm) | | |
| | Y ₂ = EE (%) | | |
| | Y ₃ = The Drug release (%) | | |

that was left behind after centrifugation. Using ultraviolet spectroscopy set at 226 nm, samples were examined. The following formulae were used to compute the NPs' EE.^{24,25}

$$\% EE = \frac{\text{Total drug-free drug}}{\text{Total drug}} \times 100 \text{ ----- (1)}$$

• Fourier transform infrared spectrum

In order to investigate potential interactions between GLMP and the excipients used in the NP as well as the stability of the drug during this process, FTIR spectroscopy was conducted¹⁹. The analysis was carried out using the potassium bromide disc method, whereby samples of approximately palletized under vacuum, 2 to 3 mg of the mixture were combined with KBr, and analyzed using an FTIR spectrophotometer (PerkinElmer, US) over a 4000 to 400 cm⁻¹ range.²⁶

• Differential scanning calorimetry

The DSC (TA Instruments US) was utilized to conduct a DSC analysis. Precisely weighed specimens were placed in aluminum pans and covered with lids.²⁷

• X-ray diffractometry

The altered crystallinity of Gliclazide upon nanonization is revealed by X-ray powder diffraction measurements using Malvern Analytical, UK.²⁸

• Scanning electron microscopy

Surface morphology and shape was investigated using scanning electron microscopy (Jeol Ltd Japan). At 15.0 kV of acceleration, the working distance was kept between 8.6 and 8.8 mm. By applying a gold coating, the nanoparticles became electrically conductive. A brass tub was used to mount these gold-coated nanoparticles using double-sided adhesive tape. The ion sputter was kept at 5 pa vacuum throughout the entire process.²⁹

• In-vitro drug release investigations

The drug dissolution investigations were conducted utilizing pH 7.4 phosphate buffer (900 mL) for both pure gliclazide and GLC nanosuspension. Each substance was separately dispersed into 3 mL of pH 7.4 phosphate buffer, and this dispersion was then filled into dialysis tubes, securely tied at both ends. These tubes were placed in a dissolution test apparatus with the release media, maintaining a temperature of 37 ± 0.5°C, and paddles working at 100 rpm. Sample aliquots (5 mL) were collected at intervals of 0, 5, 10, 15, 20,

25 and 30 minutes, sieved with a 0.45 μm membrane filter. After each collection, 5 mL of new media was introduced towards the dissolution media. The UV spectrophotometer at 226 nm was utilized to determine the amount of drug present.³⁰

RESULT AND DISCUSSION

Statistical Analysis

In a multidimensional cube, the Box-Behnken design sets a point in triplicate at the center and at the middle of each edge. Thus, in order to investigate the factors systematically, the Box Behnken design was utilized. The 17 experimental runs for the nanosuspension formulation optimization, together with all the observed responses (dependent variables). The multiple regression analysis was fitted to the responses (Y1, Y2, and Y3) to provide the linear equations suggested by the Design expert software summarized in Table 2.³¹

Response Surface Analysis

With the assistance of Design Expert Software, the model equations were employed to create the (2D) 2-dimensional contour plots and (3D) 3-dimensional response surface plots.³²

Y1 (Particle Size)

The linear equations of Y1 predicted that the sequential *p-value* is <0.0001 which is less than 0.05 and predicts the strong evidence against the null hypothesis summarized in Table 3. The R² value is 0.9710, and the adjusted and predicted R² value is 0.9643 and 0.9619 which had a difference of less than 0.2 summarized in Figure 1 and Table 3. The ANOVA equation predicts the interaction between the consistent outcome of the independent variables and the dependent variables. Thus, this equation demonstrated that the X1, X2, and X3 depict the synergistic effect on Y1. The values of X1, X2, and X3 are equally responsible for Y1. Commencing the given equation, it was summarized that increase in % concentration of X1, X2, and X3 leads to increase in particle size. Similarly, the factors that were equally responsible were visualized in contour plots and response surface plots.

Y2 (Entrapment Efficiency)

The linear equations of Y2 predicted that the sequential *p-value* is <0.0001 which is less than 0.05 and predicts the strong evidence against the null hypothesis summarized in the Table 4. The R² value is 0.8609, and the adjusted and predicted R² value is 0.8288 and 0.7740 which had a difference of less than 0.2 summarized in Figure 2 and Table 4. The ANOVA equation predicts the interaction between the consistent outcome of the independent variables and the dependent variables. Thus, this equation demonstrated that the X1, X2, and X3 depict the antagonistic effect on Y2. The values of X1, X2, and X3 are equally responsible for Y2. From the given equation, could predict the closest response of Y2. The X1, X2, and X3 factor are decreased which lead to the highest Y2 response thus, through this equation we can assume that the decrease in the amount of X1, X2, and X3 factor could lead to the ameliorated enclosed of the drug. Similarly, the factors that were equally

Table 2: Box behnken design

| Run | X1 (mg) | X2 (mg) | X3 (minutes) | Y1 (nm) | Y2 (%) | Y3 (%) |
|-----|---------|---------|--------------|---------|--------|--------|
| F1 | 105 | 115 | 20 | 273 | 88.23 | 91.1 |
| F2 | 105 | 105 | 15 | 293 | 83.98 | 84.34 |
| F3 | 115 | 115 | 15 | 353 | 79.98 | 79.67 |
| F4 | 95 | 115 | 15 | 296 | 83.12 | 84.98 |
| F5 | 105 | 105 | 15 | 312 | 81.98 | 82.12 |
| F6 | 105 | 105 | 15 | 324 | 82.56 | 83.12 |
| F7 | 95 | 105 | 10 | 313 | 83.56 | 84.67 |
| F8 | 115 | 105 | 20 | 285 | 89.86 | 92.9 |
| F9 | 105 | 115 | 10 | 378 | 78.67 | 78.34 |
| F10 | 105 | 95 | 20 | 228 | 93.89 | 96.5 |
| F11 | 95 | 105 | 20 | 224 | 95.65 | 97.8 |
| F12 | 115 | 95 | 15 | 304 | 83.76 | 85.12 |
| F13 | 105 | 105 | 15 | 297 | 86.98 | 89.12 |
| F14 | 105 | 95 | 10 | 327 | 84.63 | 85.78 |
| F15 | 105 | 105 | 15 | 297 | 84.98 | 86.13 |
| F16 | 115 | 105 | 10 | 374 | 80.12 | 81.09 |
| F17 | 95 | 95 | 15 | 239 | 91.98 | 94.9 |

Y1 = -141.14493 +3.05025*X1 +2.52500*X2 -9.55050*X3

Y2 = +129.14717 - 0.257375*X1 -0.303250*X2 +1.01625*X3

Y3 = +136.72610 -0.94625*X1 -0.352625*X2 +1.21050*X3

Table 3: Summary of regression analysis of response Y1

| Source | Sum of Squares | DF | Mean Square | F-value | p-value |
|----------|----------------|----|-------------|---------|---------|
| Model | 30786.13 | 3 | 10262.04 | 144.86 | <0.0001 |
| A-X1 | 7443.22 | 1 | 7443.22 | 105.07 | <0.0001 |
| B-X2 | 5100.50 | 1 | 5100.50 | 72.00 | <0.0001 |
| C-X3 | 18242.41 | 1 | 18242.41 | 257.51 | <0.0001 |
| Residual | 920.95 | 13 | 70.84 | | |

Table 4: Summary of regression analysis of response Y2

| Source | Sum of squares | DF | Mean square | F-value | p-value |
|----------|----------------|----|-------------|---------|---------|
| Model | 333.11 | 3 | 111.04 | 26.82 | <0.0001 |
| A-X1 | 52.99 | 1 | 52.99 | 12.80 | 0.0034 |
| B-X2 | 73.57 | 1 | 73.57 | 17.77 | 0.0010 |
| C-X3 | 206.55 | 1 | 206.55 | 49.89 | <0.0001 |
| Residual | 53.82 | 13 | 4.14 | | |

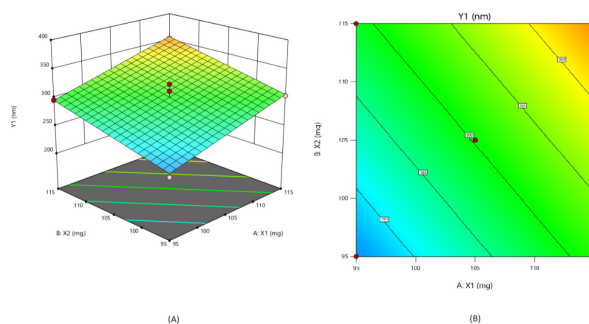


Figure 1: Response and contour plot of response Y1

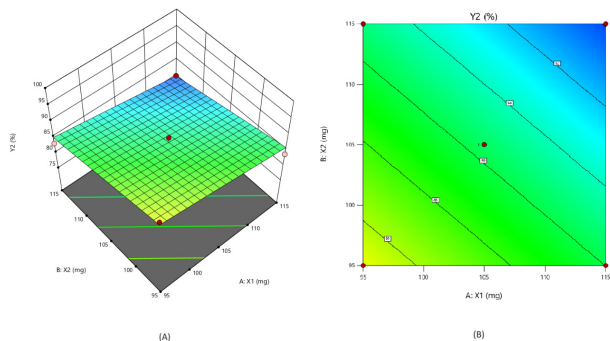


Figure 2: Response and contour plot of response Y2

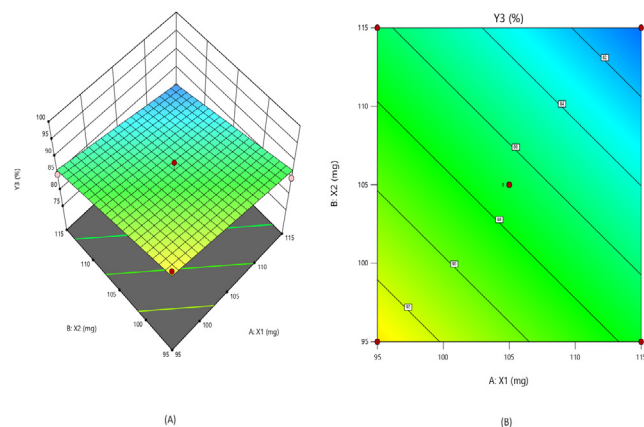


Figure 3: Response and contour plot of response Y3

Table 5: Summary of regression analysis of response Y3

| Source | Sum of Squares | DF | Mean Square | F-value | p-value |
|----------|----------------|----|-------------|---------|---------|
| Model | 461.98 | 3 | 153.99 | 22.69 | <0.0001 |
| A-X1 | 69.44 | 1 | 69.44 | 10.23 | 0.0070 |
| B-X2 | 99.48 | 1 | 99.48 | 14.66 | 0.0021 |
| C-X3 | 293.06 | 1 | 293.06 | 43.19 | <0.0001 |
| Residual | 88.22 | 13 | 6.79 | | |

Table 6: Optimization results

| S. No. | X1 | X2 | X3 | Desirability |
|--------|--------|--------|--------|--------------|
| 1. | 95.037 | 95.048 | 19.928 | 1.000 |

| Sr. No. | Response Variables | Predicted value | Actual Value | Percentage bias |
|---------|---------------------------|-----------------|--------------|-----------------|
| 1. | Particle Size (nm) | 222.74 | 221 | 0.0078 |
| 2. | Entrapment Efficiency (%) | 93.18 | 90 | 0.0341 |
| 3. | In-vitro Drug Release | 97.8 | 95.6 | 0.0224 |

responsible were visualized in contour plots and response surface plots.

Y3 (in-vitro Drug Release)

The linear equations of Y3 predicted that the sequential p-value is <0.0001 which is less than 0.05 and predicts the strong evidence against the null hypothesis summarized in the Table 5. The R²

value is 0.8397, and the adjusted and predicted R² value is 0.8027 and 0.7514 which had a difference of less than 0.2 summarized in Figure 3 and Table 5. The ANOVA equation predicts the interaction between the consistent outcome of the independent variables and the dependent variables. Thus, this equation demonstrated that the X1, X2, and X3 depict the antagonistic effect on Y3. The values of X1, X2, and X3 are equally responsible for Y3. The given equation demonstrated that the X1, X2, and X3 factors are decreased which leads to an increase in the release of the drug. Thus, we can assume that the decrease in the quantity of aspects tends towards increase the release of the drug. Similarly, the factors that were equally responsible were visualized in contour plots and response surface plots.

Validation of Optimized Condition for formulation

Numerical optimization was utilized towards determining the best values for formulation variables, resulting in a maximum desirability score of 1.000. The model demonstrated its reliability and validity as the experimental and predicted values exhibited minimal percentage bias, confirming its trustworthiness summarized in Table 6.³³

Particle size, and %EE

The size of particles and PDI were assessed utilizing the Nano ZS 90, Malvern Instruments, UK. Gliclazide-loaded nanosuspensions were found to range between 223.98 ± 1.23 nm to 378 ± 0.56 nm summarized in Figure 4. The particle size of F1 to F17 batches described in Table 6. The polydispersity index was found to be 0.198 ± 0.1 to 0.246 ± 0.02. Zeta potential of -17 mV was observed that lies within acceptable range of -30 to + 30 mV indicating excellent stability of nanosuspension

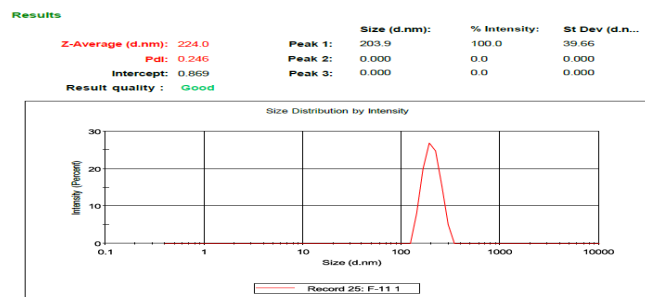


Figure 4: Particle size graph

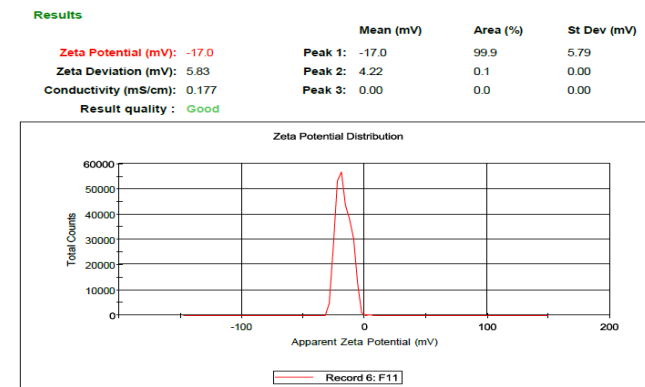


Figure 5: Zeta potential graph

(Figure 5). Moreover, the %EE was carried out through the concentration of both free and entrapped drugs assessed at the range between 78.67 ± 0.63 to $95.65 \pm 0.12\%$.³⁴

Fourier transform infrared spectrum

Utilizing the FTIR for the verification of compatibility of gliclazide with numerous polymers utilized to formulate the nanosuspension of gliclazide. The FTIR spectrum of gliclazide pure drug, and nanosuspensions were represented in Figure. However, the peaks of FTIR of pure drug gliclazide were visualized at 1704 cm^{-1} with a significant concave curve of the C=O sulfonylurea group, furthermore, at 3369 cm^{-1} represented a clear peak of the amino group, additionally, the sulfonyl group bands were observed symmetric stretching peak at 1344 and 1151.96 cm^{-1} , Moreover, the similar peaks were described in the physical mixture and in the nanosuspension. Include in the physical mixture the peak perceived at 1704 cm^{-1} (C=O sulfonylurea group), 3369.18 cm^{-1} (Amino group), and 1394.79 and 1152.15 cm^{-1} (Sulfonyl group bands). Whereas, in the nanosuspension, the peak perceived at 1704.26 cm^{-1} (C=O sulfonylurea group), 3368.71 cm^{-1} (Amino group), and 1344.25 and 1151.03 cm^{-1} (Sulfonyl group bands) summarized in Figures 6 and 7. Thus, there is no new peak was seen in the spectrum in the nanosuspensions indicating that they are constant and unaffected, and no polymorphic changes in the gliclazide during the nanosuspension creation by the numerous polymers (Koliccoat/Soluplus/SLS). In addition, the lack of changes in the peak wave number of the nanosuspensions relative to the pure drug suggest that there is no molecular interaction between the polymer and drug in nanosuspension.³⁵⁻³⁷

Differential scanning calorimetry

According to DSC thermograms (Figures 8 and 9), the gliclazide demonstrated a solitary endothermic peak at 214.36°C , whereas the other excipients that were utilized for the formation of nanosuspension include, Soluplus, SLS, and Koliccoat demonstrated the abrupt melting endotherms responses at 62.32 , 197.28 , 213.11°C which clearly state that the drug and excipient was in their crystalline state. However, the optimised formulation which contains gliclazide and other excipients demonstrated a solitary endothermic peak at 199.83°C . It represents that the gliclazide solubilizes or melts with the excipients and demonstrates the absence of crystalline form. Moreover, it is reported by numerous scientific groups that there is no visualization of gliclazide endothermic peak in the final formulation including Biswal *et al* formulated the gliclazide solid dispersions and in the result of DSC thermograms the endothermic peak of gliclazide is not visualized in the final formulation.³⁸⁻⁴⁰

X-ray diffractometry

XRD investigation was conducted towards determining the nature of a compound formed during a precipitation process, which could be either amorphous or crystalline. The analysis revealed that the XRD pattern of the pure drug closely resembled that of the crystalline form, exhibiting distinct peaks at specific diffraction angles (e.g., 14.5 – 15.5 ,

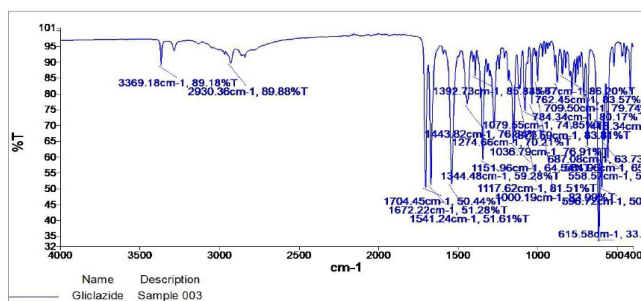


Figure 6: FTIR spectrum of drug

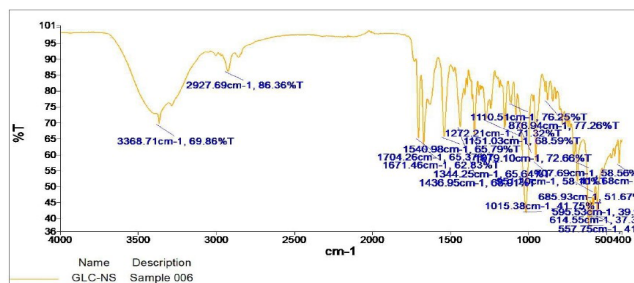


Figure 7: FTIR spectra of nanosuspension

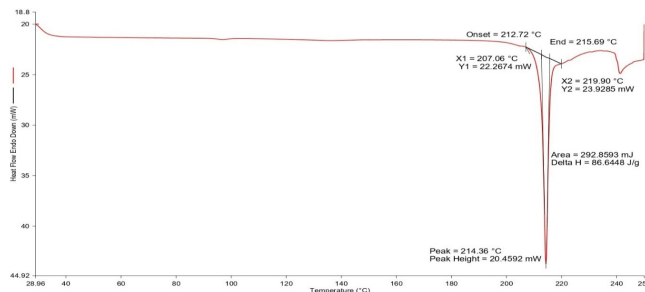


Figure 8: DSC graph of pure drug

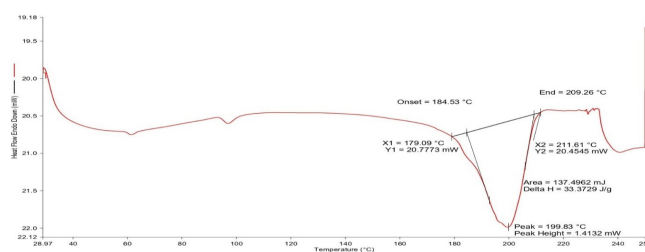


Figure 9: DSC graph of Nano-formulation

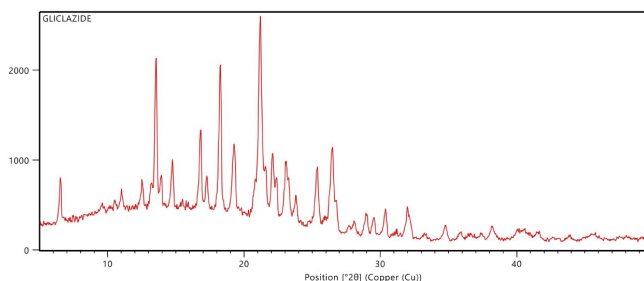


Figure 10: XRD graph of pure drug

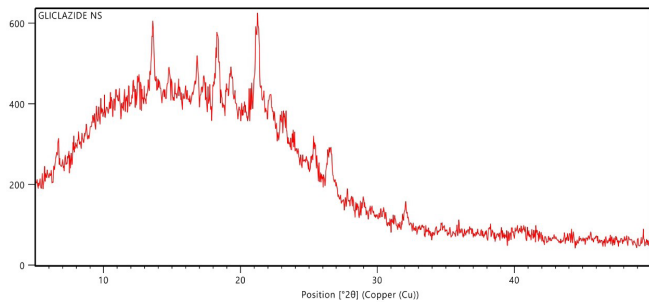


Figure 11: XRD graph of nano-formulation

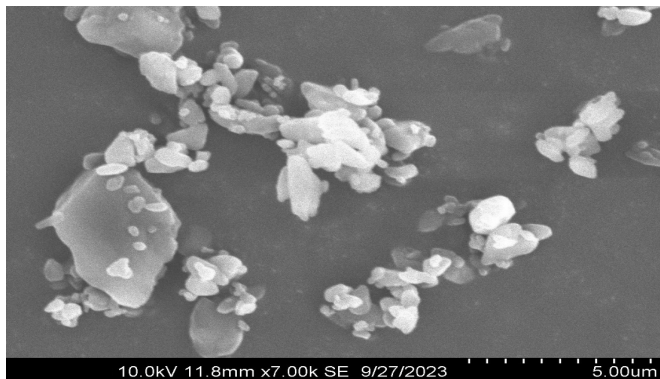


Figure 12: SEM image of pure drug

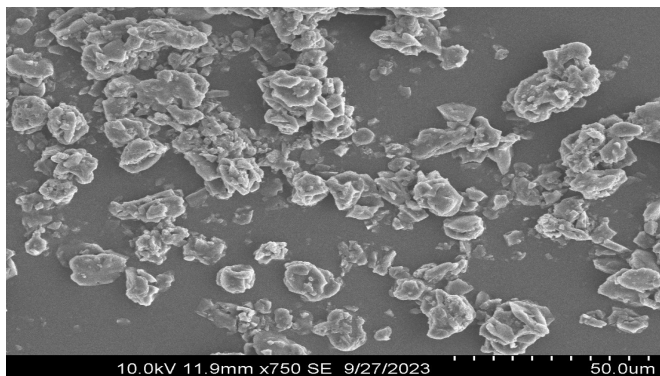


Figure 13: SEM image of nanosuspension

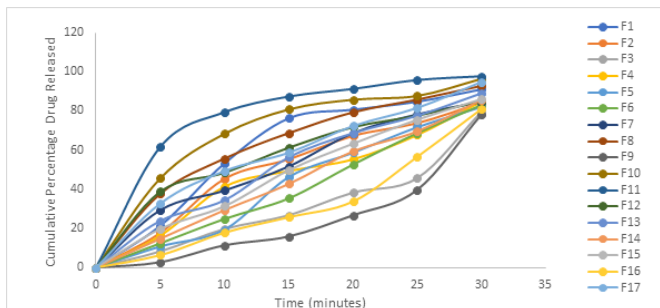


Figure 14: In-vitro release data of F1-F17

18.5–19, 21.5–22.5, 25–26, 26.5–27.5) summarized in Figures 10 and 11. While there is no similarity visualized in XRD patterns in nanosuspension formulation strongly suggests that the nanosuspension can't able to maintain the same crystalline structure as the pure-gliclazide thus, it changed

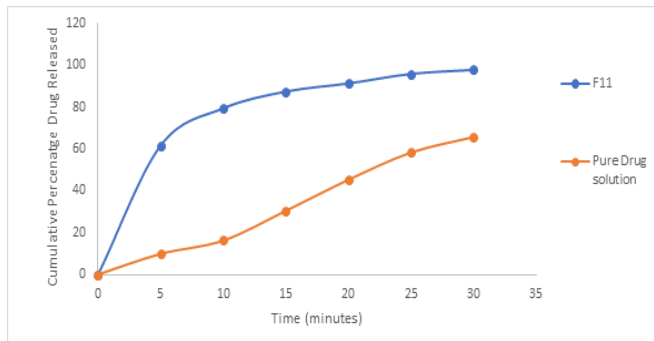


Figure 15: In-vitro release data of F11 and pure drug solution

in the amorphous form and it demonstrated that the polymer surfactant and the drug were embedded and made the proper matrix.^{41,42}

Scanning electron microscopy

The addition of polymers, surfactants, and variations in drug concentration during the process can lead to changes in the morphology of the resulting nanosuspension. The SEM imaging was employed towards examining these morphological differences summarized in Figures 12 and 13. The obtained images revealed that the nanosuspensions exhibited irregular shapes with consistent sizes and the polymer and surfactant with the drug are embedded in each other, whereas the pure gliclazide were in crystalline form, but they had non-uniform dimensions.⁴³⁻⁴⁸

In-vitro drug release study

Gliclazide-nanosuspension formulation exhibited rapid or immediate drug release during the first few minutes which visualized that more than 85% drug was released in 15 minutes. These studies were performed in dialysis bags of all 17 formulations and were found to be to $78.34 \pm 0.87\%$ to $97.8 \pm 0.90\%$ summarized in Figure 14 and 15. F11 formulation shows the significant cumulative release of the drug 97.8% release was recorded in 30 minutes. The ratio of polymer was less and surfactant as well which demonstrates the high entrapment and leads to the drug release rapidly. On the other hand, the pure drug solution released the drug, reaching nearly $30.453 \pm 0.90\%$ release within 15 minutes which is much lower than the nanosuspension formulation. In contrast, the gliclazide-nanosuspension formulation exhibited immediate release behaviour, with approximately more than 85% of the drug released within 15 minutes.⁴⁵⁻⁵¹

CONCLUSION

Gliclazide nanosuspensions formulated by the anti-solvent precipitation technique and the optimization of preparation were validated through the calculation of percentage bias which is less than 5. FTIR, DSC, and XRD visualized that the pure drug is in a crystalline system after the incorporation in nanosuspensions. The drug comes under the amorphous state. The gliclazide nanosuspensions classified the immediate release pattern which was better than the pure drug solution.

REFERENCES

- Hill-Briggs F, Adler NE, Berkowitz SA, Chin MH, Gary-Webb TL, Navas-Acien A, Thornton PL, Haire-Joshu D. Social determinants of health and diabetes: a scientific review. *Diabetes care*. 2021;44(1):258. DOI: 10.2337/dci20-0053
- Syed FZ. Type 1 diabetes mellitus. *Annals of internal medicine*. 2022;175(3):ITC33-48. DOI: 10.7326/AITC202203150
- Zhao X, An X, Yang C, Sun W, Ji H, Lian F. The crucial role and mechanism of insulin resistance in metabolic disease. *Frontiers in Endocrinology*. 2023;14:1149239. DOI: 10.3389/fendo.2023.1149239
- Naik JB, Mokale VJ, Shevkar GB, Patil KV, Patil JS, Yadava S, Verma U. Formulation and evaluation of poly (L-lactide-co-[epsilon]-caprolactone) loaded gliclazide biodegradable nanoparticles as a control release carrier. *International Journal of Drug Delivery*. 2013;(3):300.
- Tomlinson B, Patil NG, Fok M, Chan P, Lam CW. The role of sulfonyleureas in the treatment of type 2 diabetes. *Expert Opinion on Pharmacotherapy*. 2022;23(3):387-403. DOI: 10.1080/14656566.2021.1999413
- Padhi S, Nayak AK, Behera A. Type II diabetes mellitus: a review on recent drug based therapeutics. *Biomedicine & Pharmacotherapy*. 2020;131:110708. DOI: 10.1016/j.biopha.2020.110708
- Sarkar A, Tiwari A, Bhasin PS, Mitra M. Pharmacological and pharmaceutical profile of gliclazide: a review. *Journal of Applied Pharmaceutical Science*. 2011;30(Issue):11-19.
- Bolli GB, Porcellati F, Lucidi P, Fanelli CG. The physiological basis of insulin therapy in people with diabetes mellitus. *Diabetes Research and Clinical Practice*. 2021;175:108839. DOI: 10.1016/j.diabres.2021.108839
- Lv W, Wang X, Xu Q, Lu W. Mechanisms and characteristics of sulfonyleureas and glinides. *Current Topics in Medicinal Chemistry*. 2020;20(1):37-56. DOI: 10.2174/1568026620666191224141617
- Garg T, Murthy RS, Kumar Goyal A, Arora S, Malik B. Development, optimization & evaluation of porous chitosan scaffold formulation of gliclazide for the treatment of type-2 diabetes mellitus. *Drug delivery letters*. 2012;2(4):251-261. DOI: 10.2174/2210304x11202040003
- Jacob S, Nair AB, Shah J. Emerging role of nanosuspensions in drug delivery systems. *Biomaterials research*. 2020;24:1-6. DOI: <https://doi.org/10.1186/s40824-020-0184-8>
- Yadollahi R, Vasilev K, Simovic S. Nanosuspension technologies for delivery of poorly soluble drugs. *Journal of Nanomaterials*. 2015;2015:1-10. DOI: <https://doi.org/10.1155/2015/216375>
- Khandbahale SV. A review-Nanosuspension technology in drug delivery system. *Asian Journal of Pharmaceutical Research*. 2019;9(2):130-8. DOI: 10.5958/2231-5691.2019.00021.2
- Chougule M, Sirvi A, Saini V, Kashyap M, Sangamwar AT. Enhanced biopharmaceutical performance of brick dust molecule nilotinib via stabilized amorphous nanosuspension using a facile acid-base neutralization approach. *Drug Delivery and Translational Research*. 2023;6:1-7. DOI: 10.1007/s13346-023-01334-7
- Kolimi P, Narala S, Youssef AA, Nyavanandi D, Dudhipala N. A systemic review on development of mesoporous nanoparticles as a vehicle for transdermal drug delivery. *Nanotheranostics*. 2023;7(1):70. DOI: 10.7150/ntno.77395
- Müller RH, Benita S, Bohm B, editors. *Emulsions and nanosuspensions for the formulation of poorly soluble drugs*. CRC Press; 1998.
- Zhang X, Xing H, Zhao Y, Ma Z. Pharmaceutical dispersion techniques for dissolution and bioavailability enhancement of poorly water-soluble drugs. *Pharmaceutics*. 2018;10(3):74. DOI: 10.3390/pharmaceutics10030074
- Sampathi S, Prajapati S, Junnuthula V, Dyawanapelly S. Pharmacokinetics and anti-diabetic studies of gliclazide nanosuspension. *Pharmaceutics*. 2022;14(9):1947. DOI: 10.3390/pharmaceutics14091947
- Taneja S, Shilpi S, Khatri K. Formulation and optimization of efavirenz nanosuspensions using the precipitation-ultrasonication technique for solubility enhancement. *Artificial cells, nanomedicine, and biotechnology*. 2016;44(3):978-984. DOI: 10.3109/21691401.2015.1008505
- Xia D, Quan P, Piao H, Piao H, Sun S, Yin Y, Cui F. Preparation of stable nitrendipine nanosuspensions using the precipitation-ultrasonication method for enhancement of dissolution and oral bioavailability. *European Journal of Pharmaceutical Sciences*. 2010;40(4):325-334. DOI: 10.1016/j.ejps.2010.04.006
- Liu D, Xu H, Tian B, Yuan K, Pan H, Ma S, Yang X, Pan W. Fabrication of carvedilol nanosuspensions through the anti-solvent precipitation-ultrasonication method for the improvement of dissolution rate and oral bioavailability. *Aaps PharmSciTech*. 2012;13:295-304. DOI: 10.1208/s12249-011-9750-7
- Kassem MA, ElMeshad AN, Fares AR. Enhanced solubility and dissolution rate of lacidipine nanosuspension: formulation via antisolvent sonoprecipitation technique and optimization using Box-Behnken design. *AAPS PharmSciTech*. 2017;18:983-996. DOI: 10.1208/s12249-016-0604-1
- Hao J, Gao Y, Zhao J, Zhang J, Li Q, Zhao Z, Liu J. Preparation and optimization of resveratrol nanosuspensions by antisolvent precipitation using Box-Behnken design. *Aaps PharmSciTech*. 2015;16:118-28. DOI: 10.1208/s12249-014-0211-y
- Patel GV, Patel VB, Pathak A, Rajput SJ. Nanosuspension of efavirenz for improved oral bioavailability: formulation optimization, in vitro, in situ and in vivo evaluation. *Drug development and industrial pharmacy*. 2014;40(1):80-91. DOI: 10.3109/03639045.2012.746362
- Song X, Zhao Y, Hou S, Xu F, Zhao R, He J, Cai Z, Li Y, Chen Q. Dual agents loaded PLGA nanoparticles: systematic study of particle size and drug entrapment efficiency. *European journal of pharmaceutics and biopharmaceutics*. 2008;69(2):445-453. DOI: 10.1016/j.ejpb.2008.01.013
- Kalvakuntla S, Deshpande M, Attari Z, Kunnatur K. Preparation and characterization of nanosuspension of aprepitant by H96 process. *Advanced Pharmaceutical Bulletin*. 2016;6(1):83. DOI: 10.15171/apb.2016.013
- Gera S, Talluri S, Rangaraj N, Sampathi S. Formulation and evaluation of naringenin nanosuspensions for bioavailability enhancement. *Aaps PharmSciTech*. 2017;18:3151-62. DOI: 10.1208/s12249-017-0790-5
- Gulsun T, Bornha SE, Vural I, Sahin S. Preparation and characterization of furosemide nanosuspensions. *Journal of Drug Delivery Science and Technology*. 2018;45:93-100. DOI: 10.1016/j.jddst.2018.03.005
- Ravouru N, Venna RS, Penjuri SC, Damineni S, Kotakadi VS, Poreddy SR. Fabrication and characterization of gliclazide nanocrystals. *Advanced Pharmaceutical Bulletin*. 2018;8(3):419. DOI: 10.15171/apb.2018.049
- Mudgil M, Pawar PK. Preparation and in vitro/ex vivo evaluation of moxifloxacin-loaded PLGA nanosuspensions for ophthalmic

- application. *Scientia pharmaceutica*. 2013;81(2):591-606. DOI: 10.3797/scipharm.1204-16
31. Porwal O. Box-Behnken Design-based formulation optimization and characterization of spray dried rutin loaded nanosuspension: State of the art. *South African Journal of Botany*. 2022;149:807-815. DOI: 10.52711/0974-360X.2022.00244
 32. Nagaraj K, Narendar D, Kishan V. Development of olmesartan medoxomil optimized nanosuspension using the Box–Behnken design to improve oral bioavailability. *Drug development and industrial pharmacy*. 2017;43(7):1186-1196. DOI: 10.1080/03639045.2017.1304955
 33. Kassem MA, ElMeshad AN, Fares AR. Enhanced solubility and dissolution rate of lacidipine nanosuspension: formulation via antisolvent sonoprecipitation technique and optimization using Box–Behnken design. *AAPS PharmSciTech*. 2017;18:983-996. DOI: 10.1208/s12249-016-0604-1
 34. Borkhataria C, Patel D, Bhagora S, Patel N, Patel K, Manek R. Study of homogenization on media milling time in preparation of irbesartan nanosuspension and optimization using design of experiments (DoE). *Future Journal of Pharmaceutical Sciences*. 2020;6(1):1-2. DOI: <https://doi.org/10.1186/s43094-020-00105-2>
 35. Ali HR, Saleh GA, Hussein SA, Hassan AI. In-depth qualitative and quantitative FTIR spectroscopic study of glipizide and gliclazide. *Analytical Chemistry: An Indian Journal*. 2014;14(4):127-134.
 36. Padmavathi Y, Anjali A, Babu NR, Kumar PR. Development and validation of new FTIR method for quantitative analysis of gliclazide in bulk and pharmaceutical dosage forms. *Asian Journal of Research in Chemistry*. 2017;10(3):377-382. DOI: 10.13040/IJPSR.0975-8232.11(2).862-72
 37. Sunitha PG, Deattu N, Balachandar C, Nandhini P, Narayane R, Kavitha MS, Sivakumar D. FTIR spectroscopic method for quantitative analysis of gliclazide in tablets. *Journal of Drug Delivery and Therapeutics*. 2014;4(3):145-160. DOI: <https://doi.org/10.22270/jddt.v4i3.872>
 38. Biswal S, Sahoo J, Murthy PN, Giradkar RP, Avari JG. Enhancement of dissolution rate of gliclazide using solid dispersions with polyethylene glycol 6000. *Aaps Pharmscitech*. 2008;9(2):563-570. DOI: 10.1208/s12249-008-9079-z
 39. Jondhale S, Bhise S, Pore Y. Physicochemical investigations and stability studies of amorphous gliclazide. *Aaps Pharmscitech*. 2012;13:448-459. DOI: 10.1208/s12249-012-9760-0
 40. Solunke RS, Borge UR, Murthy K, Deshmukh MT, Shete RV. Formulation and evaluation of gliclazide nanosponges. *International Journal of Applied Pharmaceutics*. 2019;11(6):181-189. DOI: 10.22159/ijap.2019v11i6.35006
 41. Rajamma AJ, Sateesha SB, Narode MK, Prashanth VR, Karthik AM. Preparation and crystallographic analysis of gliclazide polymorphs. *Indian Journal of Pharmaceutical Sciences*. 2015;77(1):34. DOI: 10.4103/0250-474x.151595
 42. Febriyenti F, Rahmi S, Halim A. Study of gliclazide solid dispersion systems using PVP K-30 and PEG 6000 by solvent method. *Journal of pharmacy & bioallied sciences*. 2019;11(3):262. DOI: 10.4103/jpbs.JPBS_87_18
 43. Bruni G, Berbenni V, Maggi L, Mustarelli P, Friuli V, Ferrara C, Pardi F, Castagna F, Girella A, Milanese C, Marini A. Multicomponent crystals of gliclazide and tromethamine: preparation, physico-chemical, and pharmaceutical characterization. *Drug Development and Industrial Pharmacy*. 2018;44(2):243-250. DOI: 10.1080/03639045.2017.1386208
 44. Ayon NJ, Hasan I, Islam MS, Reza MS. Preparation and characterization of gliclazide incorporated cellulosic microspheres: studies on drug release, compatibility and micromeritics. *Dhaka University Journal of Pharmaceutical Sciences*. 2014;13(2):149-166. DOI: 10.3329/dujps.v13i2.21893
 45. Ibrahim MA, Shazly GA, Aleanizy FS, Alqahtani FY, Elosaily GM. Formulation and evaluation of docetaxel nanosuspensions: In-vitro evaluation and cytotoxicity. *Saudi pharmaceutical journal*. 2019;27(1):49-55. DOI: 10.1016/j.jsps.2018.07.018
 46. He S, Yang H, Zhang R, Li Y, Duan L. Preparation and in vitro–in vivo evaluation of teniposide nanosuspensions. *International journal of pharmaceutics*. 2015;478(1):131-137. DOI: 10.1016/j.ijpharm.2014.11.020
 47. Sahoo CK, Mishra AK, Moharana AK. Formulation and Evaluation of Carbamazepine Nanosuspension with the Help of Cosolvent Technique. *International Journal of Drug Delivery Technology*. 2022;12(2):472-475. DOI: 10.25258/ijddt.12.2.2.
 48. Naik DCS, Bharathi A. 23 Full Factorial Designs for Formulation and Evaluation of Non-Steroidal Anti-inflammatory Drug. *International Journal of Drug Delivery Technology*. 2022;12(1):1-7. DOI: 10.25258/ijddt.12.1.1.
 49. Moinuddin, Neekhara S, Ahmad S, Swarnkar SK, Gupta D, Khunteta A, Jain P, Jain S. Evaluation of Oral Bioavailability and In-vivo Anti-leukemic Potential of Dasatinib Loaded Solid Lipid Nanoparticles. *International Journal of Pharmaceutical Quality Assurance*. 2023;14(3):587-591. DOI: 10.25258/ijpqa.14.3.21.
 50. Mamatha P, Bhikshapathi DVRN. Preparation and In-vitro Evaluation of Pemigatinib Nanosponges Tablets by Box-Behnken Design. *International Journal of Pharmaceutical Quality Assurance*. 2023;14(3):791-800. DOI: 10.25258/ijpqa.14.3.56.
 51. Bhilare NV, Marulkar VS, Kumar D, Chatap VK, Patil KS, Shirote PJ. An insight into prodrug strategy for the treatment of Alzheimer’s disease. *Medicinal Chemistry Research*. 2022 Mar;31(3):383-99. <https://doi.org/10.1007/s00044-022-02859-1>